2011

# Northeast US precipitation variability and North American climate teleconnections interpreted from late Holocene varved sediments

J. Bradford Hubeny

John W. King
*University of Rhode Island*, jwking@uri.edu

***See next page for additional authors***



Citation/Publisher Attribution

Hubenym J. B., King, J. W., & Reddin, M. (2011). Northeast US precipitation variability and North American climate teleconnections interpreted from late Holocene varved sediments. *Proc Natl Acad Sci USA, 108*(44), 17895-17900. doi: 10.1073/pnas.1019301108
Available at: http://dx.doi.org/10.1073/pnas.1019301108

# Northeast US precipitation variability and North American climate teleconnections interpreted from late Holocene varved sediments

J. Bradford Hubeny[a,1], John W. King[b], and Mike Reddin[a]

[a]Department of Geological Sciences, Salem State University, 352 Lafayette Street, Salem, MA 01970; and [b]Graduate School of Oceanography, University of Rhode Island, Narragansett, RI 02882

Edited by Ray S. Bradley, University of Massachusetts, Amherst, MA, and accepted by the Editorial Board September 9, 2011 (received for review December 21, 2010)

**A more thorough understanding of regional to hemispheric hydroclimate variability and associated climate patterns is needed in order to validate climate models and project future conditions. In this study, two annually laminated (varved) sediment records spanning the last millennium were analyzed from Rhode Island and New York. Lamination thickness time series from the two locations are significantly correlated to hydroclimate indicators over the period of instrument overlap, demonstrating their usefulness in reconstructing past conditions. Both records are correlated to climate teleconnection indices, most strongly the Pacific/North American (PNA) pattern, suggesting regional to hemispheric influences on hydroclimate. Such a linkage is interpreted to be due to tropospheric circulation patterns in which positive PNA periods are associated with meridional circulation, leading to the dominance of southern moist air masses in the Northeast United States. Alternatively, the zonal flow over North America associated with negative PNA periods produces dominant dry continental air masses over the region. A composite record from the two locations reveals variability of hydroclimate and atmospheric circulation over the late Holocene and shows similarities to previously published reconstructions of the circumpolar vortex and of the Aleutian Low-pressure system, supporting the hypothesized PNA linkage. The record is correlated to continental-scale droughts, many of which have been reconstructed in the American Southwest. These results demonstrate the PNA's influence on hydroclimate over North America, and suggest that this teleconnected pattern may have a significant role in continental drought dynamics.**

Green Lake | Pettaquamscutt River Estuary | Quaternary | New England | paleolimnology

Hydroclimate variability affects water resources, flood frequency, human health, economic activity, ecosystem functions, and has a positive feedback with atmospheric warming (1, 2). The water cycle is intensifying, however uncertainties remain due to regional variability, gaps in spatial data coverage, and temporal limitations (3, 4). Although modeling studies have made progress predicting future changes to the hydrologic cycle (5), regional anomalies, an incomplete understanding of the driving mechanisms, and a lack of high-resolution paleo-data (6) make it difficult to validate models.

The Northeast United States (NE), which has a large population and active agriculture, is prone to both flood hazards (7) and soil, meteorological, and hydrological droughts (8). Over the last century, winter precipitation in the NE has increased by 10–15%, likely due to natural variability in the climate system (9). Simulations project that winter precipitation in the NE will likely continue to increase by 20–30% by the end this century (10), suggesting an acceleration of the current trend of hydroclimate intensification in the NE.

Hydroclimate variability is influenced by atmospheric circulation patterns, often described by teleconnection indices (6, 11). A more thorough understanding of regional hydroclimate variability and the associated linkages to known hemispheric/global patterns may assist in future predictive capabilities throughout North America. The patterns of atmospheric pressure centers described by these indices influence hydroclimatology by modulating midtropospheric circulation patterns and storm tracking (12). An important reconstruction of the position and amplitude of the vortex trough in the NE over the past millennium demonstrated that this dominant atmospheric feature has influenced precipitation variability over the late Holocene (13). A more complete understanding of the processes that are controlling hydroclimate variability in the NE will be applicable in other regions such as the American Southwest (SW) that are affected by the same teleconnection patterns.

In this study, two varved sediment records from the NE were utilized to investigate hydroclimate variability in the region over the past millennium. Specifically, we aim to: (*i*) document late Holocene precipitation variability in the NE; (*ii*) assess the teleconnection influences on such variability; (*iii*) generate a composite record of regional variability in NE hydroclimate variability and associated atmospheric circulation patterns; and (*iv*) assess the record in light of previously constructed North American hydroclimate (drought) records.

## Study Locations

The Pettaquamscutt River Estuary (PR), Rhode Island (RI), and Green Lake (GL), New York (NY) were selected for this study based on the following: (*i*) both locations contain varved sediments that afford robust age models (chronologic error <1%); (*ii*) neither location appears to have a major anthropogenic overprint on the sedimentary record (*SI Text*, *Table S1*); (*iii*) both locations are sensitive to climate variability; and (*iv*) the two locations represent east and west endmembers of a transect across the NE region (Fig. 1). The PR's Lower Basin is an ice block depression that has been inundated by marine waters, leading to stable density stratification (14), anoxic bottom waters, and preservation of varved sediments (15). Each varve is composed of a biogenic layer deposited after the annual phytoplankton bloom and a siliciclastic layer that is deposited during the remainder of the year, likely as a result of sediment transport via runoff from the watershed (16). Additional transport mechanisms are likely (i.e., eolian, wave, and current transport), however the relative importance of each is difficult to quantify due to a lack of historic data of these variables. Fossil pigments associated with the biogenic portion of the varved sediments have previously

Author contributions: J.B.H. and J.W.K. designed research; J.B.H. and M.R. performed research; J.B.H., J.W.K., and M.R. analyzed data; and J.B.H. wrote the paper.

The authors declare no conflict of interest.

This article is a PNAS Direct Submission. R.S.B. is a guest editor invited by the Editorial Board.

[1]To whom correspondence should be addressed. E-mail: bhubeny@salemstate.edu.

This article contains supporting information online at www.pnas.org/lookup/suppl/doi:10.1073/pnas.1019301108/-/DCSupplemental.



GEOLOGY

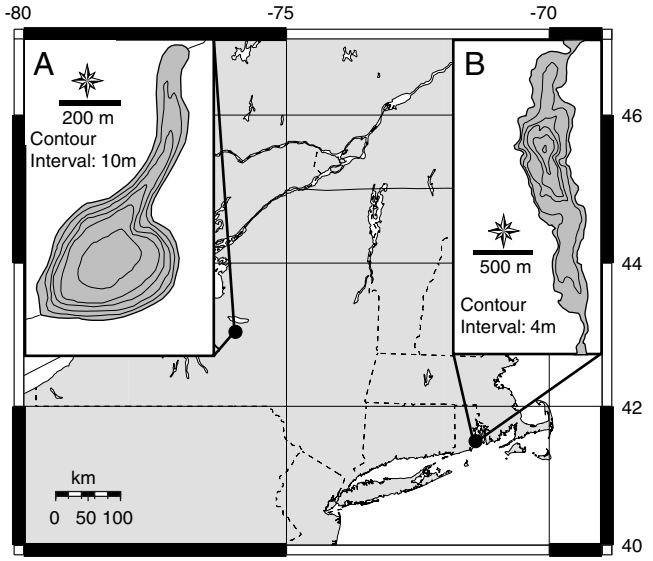


**Fig. 1.** Locus map of the Northeast US showing GL (*A*) and the PR (*B*). Sediment cores were taken from the deepest region of each water body.

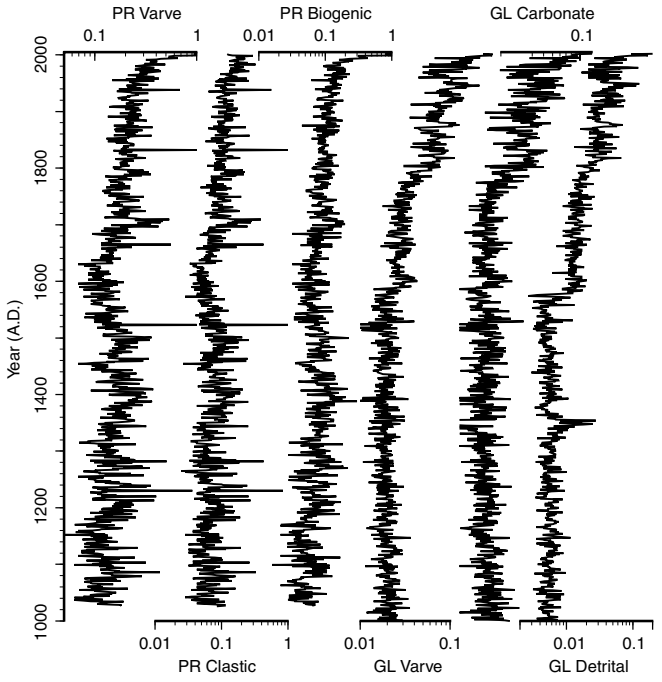


**Fig. 2.** Varve and lamination thickness time series for PR and GL sediments over the past millennium. See text (*Study Locations*) for compositonal descriptions of laminations. All thicknesses are composite thicknesses (cm) from multiple cores and have been corrected for differential compaction.

been shown to correlate with North Atlantic climatic parameters through a temperature control on bacterial autotrophs (15).

GL has been extensively studied over the last few decades due to its unique physical and chemical conditions. Permanent stratification and varve preservation (17) is observed due to the small surface area to depth ratio as well as the influx of saline groundwater at depth (18). The influx of calcium ions from groundwater leads to episodes of supersaturation and precipitation of calcite in the water column (19) where *Synechococcus* serve as nucleation sites (20). Each varve contains a calcite layer and a darker detrital layer consisting of clastic and terrigenous organic material. Massive and graded laminations and beds have been identified as turbidites throughout the lake (21).

## Results and Discussion

**Core Lithologies and Age Models.** ***Pettaquamscutt River.*** The stratigraphy of the upper *ca.* 2 m from the PR's Lower Basin consists of an upper finely laminated, organic-rich mud facies and a lower massive, organic-rich mud facies below *ca.* 1.9 m. Laminations have been demonstrated to form annually through independently determined age constraints (15, 22) (ftp://rock.geosociety.org/pub/reposit/2006/2006109.pdf). The average sedimentation rate for this varved section of sediment was 1.8 mm/y (Fig. 2). Both high- and low-frequency signals are observed in the time series, likely reflecting past variability of sedimentation associated with atmospheric as well as oceanic influences (15).

***Green Lake.*** Sediment cores from GL contain finely laminated, carbonate-rich mud. Laminations alternate between light (carbonate) and dark (detrital) materials, with intermittent turbidites up to 3 cm thick. Previous studies have demonstrated that the laminations in GL are formed annually, and are therefore varves (17, 21, 23). The annual nature of the laminations is supported by an observed increased sedimentation rate for sediments deposited since *ca.* 1800 A.D., consistent with previous studies using radiometric age controls (24). The average sedimentation rate of the varved sediments is 0.4 mm/y, with rates of 0.2 and 1.0 mm/y before and after 1800 A.D., respectively (Fig. 2). An increase in the thickness of detrital laminations was observed at *ca.* 1600 A.D., however the cause of this shift remains unclear.

**Varve Preservation of Hydroclimate Variability.** ***Pettaquamscutt River.*** Significant relationships are noted between PR lamination thicknesses and RI hydroclimate data (Table 1). First, correlations between PR clastic lamination thicknesses (PRCL) and both precipitation and Palmer Drought Severity Index (PDSI) were very strong for both the annual and decadally smoothed time series ($p < 0.001$), suggesting that the thicknesses of clastic laminations from the PR have preserved hydrologically forced variability for the region. Additionally, surface air temperatures are statistically correlated to PRCL thicknesses, albeit with lesser confidence ($p = 0.017$). The organic lamination thicknesses correlate significantly with precipitation, but not PDSI, and the correlations are weaker than those found for the clastic laminations. Higher significance values are observed between the organic laminations and surface air temperature, which is consistent with previous interpretations that organic laminations are composed of amorphous biogenic material deposited after seasonal water column blooms, and that the productivity that this lamination represents is partially forced by thermal controls on the autotrophs in the water column (15, 16).

More information was obtained regarding the mechanism of PRCL formation by regressing the clastic lamination thickness time series to seasonal precipitation totals (25). The strongest correlations were observed in the winter and spring months (decadally smoothed: $r = 0.71$ and 0.76, respectively), suggesting that the underlying mechanism controlling much of the precipitation variability in RI is occurring during these months. This result was consistent with the varve formation model documented by Lincoln, et al. (16), in which the dark biogenic layer is deposited as organic matter settles through the water column during and after the annual primary-producer bloom.

***Green Lake.*** GL carbonate lamination (GLCL) thicknesses correlate significantly and positively with both precipitation and PDSI at both annual and decadal time scales (Table 1). Examination of seasonal correlations reveals that the strongest correlation with precipitation occurs during the summer season ($r = 0.27$) (25). Summer corresponds with the timing of *Synechococcus* blooms, which trigger carbonate precipitation in the water column (20).

**Table 1. Correlation tests between PR and GL compaction-corrected varve/lamination thicknesses versus regional climate variables from RI and NY, respectively**

| Climate variable | PR varve | PR clastic lamination | PR biogenic lamination | GL varve | GL carbonate lamination | GL detrital lamination |
|---|---|---|---|---|---|---|
| Precipitation (annual) | 0.36* | 0.45* | 0.20‡ | 0.28† | 0.37* | 0.08 |
| Precipitation (decadal) | 0.69* | 0.84* | 0.48‡ | 0.42‡ | 0.53† | 0.12 |
| Palmer Drought Severity Index (annual) | 0.30† | 0.43* | 0.07 | 0.30† | 0.37* | 0.10 |
| Palmer Drought Severity Index (decadal) | 0.61† | 0.83* | 0.37 | 0.54† | 0.58† | 0.27 |
| Surface air temperature (annual) | 0.43* | 0.23‡ | 0.40* | 0.07 | 0.11 | 0.00 |
| Surface air temperature (decadal) | 0.53† | 0.48‡ | 0.49‡ | 0.39 | 0.40‡ | 0.11 |

*$p < 0.0001$;
†$p < 0.01$;
‡$p < 0.05$

Additionally, correlation analyses with decadally smoothed PDSI data exhibit significant correlations with fall, winter, and spring seasons ($r = 0.59$, 0.55,. and 0.55, respectively). These seasons predate the annual summer *Synechococcus* bloom, which is likely a result of the delayed transport of water to the lake due to annual snow pack.

The positive relationship between GLCL deposition and hydroclimate is likely a result of variability in groundwater input to the lake. Calcium ions are introduced to GL via groundwater (18). During negative precipitation/PDSI anomalies, groundwater recharge will decrease with a concurrent decline in $Ca^{2+}$ supply. Carbonate precipitation will then be limited by the availability of $Ca^{2+}$, and total precipitation of carbonate is reduced. This mechanism has been observed in other groundwater-dominated lakes (26).

Surface air temperatures are also significantly correlated to carbonate accumulation on decadal time scales (Table 1). The correlation could be due to either the temperature control on carbonate solubility, or its influence on metabolic activity, which would increase the efficiency of carbonate precipitation in GL.

Results of correlation analyses reveal that both PRCL and GLCL time series statistically correlate to regional hydroclimate variables. The most statistically significant correlations are associated with PDSI/precipitation vs. PRCL thicknesses and vs. GLCL thicknesses. In the subsequent sections, these two time series will be utilized to examine variability in hydroclimate conditions.

**Linkages to Northern Hemisphere Teleconnection Patterns.** Because regional climate is often associated with regional to global teleconnection patterns, it is likely that the variability observed in lamination thickness and hydroclimate are linked to such patterns. Here, the PRCL and GLCL, which are statistically representative of hydroclimate in RI and NY, respectively, were compared to climate teleconnection patterns with hypothesized influence in the NE (Table 2). Specifically, correlations were tested between lamination thicknesses and the Pacific/North American (PNA) pattern, the Northern Annular Mode (NAM), and the Southern Oscillation Index (SOI), all indices associated with winter circulation patterns in the Northern Hemisphere (6, 11).

The PNA index (December–May) exhibited the strongest correlations to PRCL and GLCL time series (Table 2). Correlations to the NAM (previous November–December) were statistically significant at interannual and decadal time scales for PRCL, and at decadal time scales for GLCL. Correlations with the SOI were significant (negative) at decadal time scales for both locations. The SOI correlations may be related to the PNA correlations due to their common Pacific linkage.

In order to put these correlations in context, it is necessary to discuss the mechanisms by which teleconnection patterns can influence precipitation in the NE. The dominant air masses that enter the NE are dry continental air, moist Gulf of Mexico air, and moist Atlantic coastal air masses (27). The most straightforward mechanism for altering the dominant air mass is by shifting from zonal to meridional tropospheric flow, thereby moving from dry continental dominance to moist Gulf of Mexico and/or moist Atlantic coastal air masses. The PNA has a strong influence on the nature of tropospheric circulation, with positive index years associated with meridional flow, and negative index years associated with zonal flow (28).

In the case of ENSO, El Niño years (SOI $< -1$) result in above normal sea surface temperatures (SSTs) in the eastern tropical Pacific Ocean. A warm tropical and cool midlatitude Pacific Ocean is associated with positive PNA index years (29, Fig. S1), and because SSTs in the Pacific partially drive the PNA (29), it is possible that strongly negative SOI states (and warm SSTs in the eastern tropical Pacific Ocean) are related to the initiation of positive PNA conditions.

The NAM has a positive correlation with winter temperatures in the NE (30). Because the correlation to the NAM is found with the previous November and December to the year of deposition, it appears that a thermal set up in winters with high NAM index (warmer) lead to a lower percentage of ice-covered days. In the case of the PR, this allows more days with active surface runoff. Warmer fall and winter temperatures in GL likely increase the precipitation of carbonate through temperature solubility controls.

**Composite Record of Regional Variability.** ***Verification.*** The PRCL and GLCL time series both correlate well with the PNA teleconnection climate pattern (Table 2). The series are also significantly correlated to each other ($r = 0.42$, $p < 0.001$; $r = 0.62$, $p < 0.001$, annual and decadally smoothed series, respectively). By combining the two time series into a composite record (see *Methods*), we can examine regional hydroclimate variability for the NE region and teleconnected variability in North America by amplifying regional signals and suppressing local climate and watershed variables influences.

The composite PRGL (PRGL) Varve Index exhibits significant temporal correlations to teleconnection patterns over the period of instrumental overlap (Table 2). The PRGL Index is especially well correlated to the PNA pattern ($r = 0.65, p < 0.001; r = 0.96$,

**Table 2. Correlation tests between climate teleconnection patterns versus PR lamination thicknesses, GL lamination thicknesses, and the PRGL Composite Varve Index**

| Teleconnection Index | PR clastic lamination | GL carbonate lamination | PRGL composite |
|---|---|---|---|
| PNA (DJFMAM)(annual) | 0.54* | 0.50* | 0.65* |
| PNA (DJFMAM)(decadal) | 0.86* | 0.88* | 0.96* |
| NAM (previous ND) (annual) | 0.28† | 0.13 | 0.24 |
| NAM (previous ND) (decadal) | 0.82* | 0.81* | 0.89* |
| SOI (annual) | −0.14 | 0.00 | −0.08 |
| SOI (decadal) | −0.51† | −0.45† | −0.54† |

*$p < 0.001$;
†$p < 0.01$;

GEOLOGY

$p < 0.001$, annual and decadally smoothed series, respectively), demonstrating the significant influence of this hemispheric teleconnection pattern over the period of instrumental overlap (Table 2 and Fig. 3*A*).

The geo-spatial pattern of atmospheric mass is also correlated between the PRGL Index and the PNA pattern. Fig. 3*B* displays correlation analyses between gridded 500 mbar height anomalies in the Northern Hemisphere and the PNA pattern. Note the strong correlations between the Aleutian Low-pressure system and the North American high-pressure system and the PNA pattern, which are strong during positive PNA index years and weak during negative PNA index years. Conducting the same analysis with the PRGL time series results in a similar pattern of spatial correlation between the reconstruction and the dominant pressure systems associated with the PNA pattern (Fig. 3*C*). Finally, a frequency domain connection is clear through the results of spectral analysis of the PRGL Index (*SI Text*). A dominant periodic component centered at 3.4 y is consistent with spectral analyses of PNA instrumental records (Fig. S2).

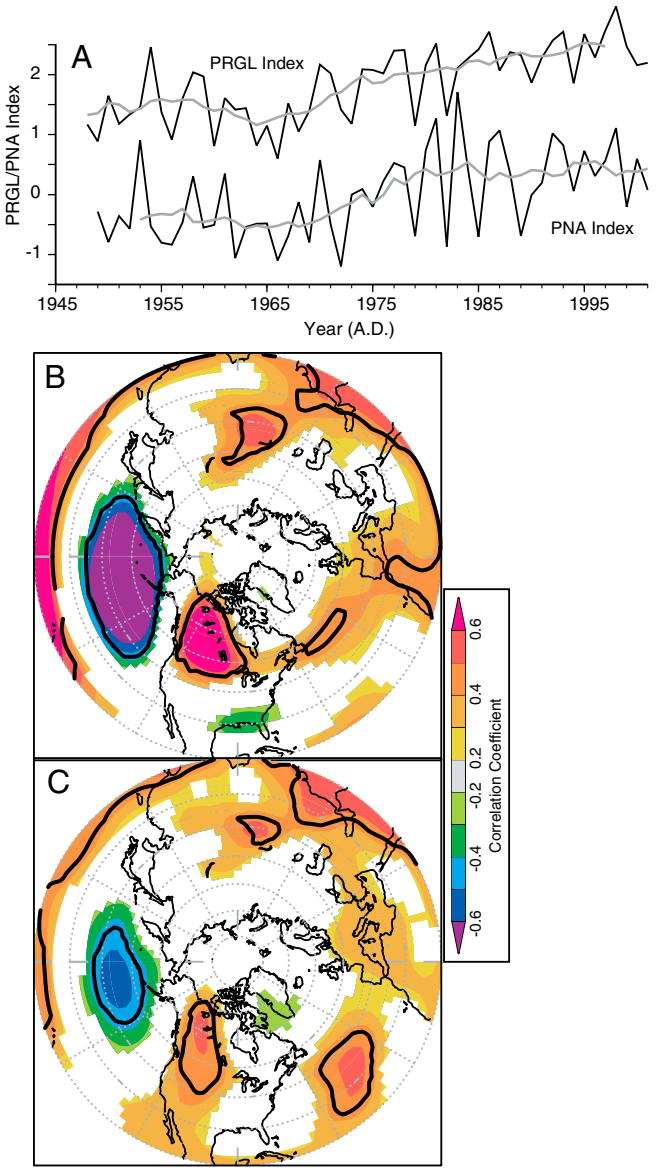


**Fig. 3.** (*A*), Composite PRGL lamination thickness record (top) and PNA Winter/Spring Index (bottom) plotted over the record of overlap. Black curves are annual data, and gray curves are decadally smoothed series. Note the high significance between the annual ($r = 0.65$; $p < 0.001$) and smoothed ($r = 0.96$; $p < 0.001$) records. Geo-spatial similarities with gridded hemispheric 500 mbar height anomalies are apparent between (*B*). Correlation analyses between the PNA index (EOF2) and gridded 500 mbar height anomalies, and (*C*). Correlation analyses between the PRGL record and gridded 500 mbar height anomalies over the period 1948–2001. Color scale indicates correlation coefficient ($r$), and thick contour shows $p = 0.001$. Note the significant correlations calculated for both series in relation to the Aleutian Low (negative) as well as the North American High (positive) pressure systems.

***PNA/Atmospheric circulation record.*** The PRGL Index is plotted in Fig. 4. Based on the verification of the record, high values are associated with positive PNA index values, and hence dominantly meridional tropospheric circulation over North America. Alternatively, low values are associated with negative PNA index values, and dominantly zonal tropospheric circulation. Variability is noted at low and high frequencies (Fig. 4, Fig. S2), suggesting that tropospheric circulation during the last millennium has been dynamic.

Because the PRGL record is indicative of regional to hemispheric atmospheric circulation patterns, the record should correlate with lower resolution records of atmospheric circulation. Kirby, et al. (13) reconstructed the winter vortex over the NE based on oxygen isotope data from GL, where an expanded vortex is related to a positive PNA pattern, and vice versa. A comparison of this record to the PRGL index, exhibits many common peaks and troughs between the records (Fig. 4). It is interesting to note, however, a lack of lower-frequency strength in the Kirby reconstruction as compared to the PRGL record.

The PRGL record should also show common patterns of variability to those of the Aleutian Low, because this low-pressure system is fundamental to the PNA atmospheric pattern (Fig. 3*B*). A reconstruction of the Aleutian Low (31) reveals variability in the strength of the Aleutian Low that correlates well with low-frequency PRGL variability (Fig. 4).

An increasing trend is noted in the PRGL index values over the past 1.5 centuries. This observation is similar to an increased trend in snow accumulation at Mt. Logan, AK, which has been attributed to changes in the PNA pattern (32). Both records show that the recent high values are anomalous in comparison to the respective periods of data coverage.

***Continental drought teleconnections.*** Due to known teleconnected climate variability associated with the PNA (11, 28, 33), the PRGL record likely has relevance for hydrologically sensitive regions outside of the NE. We tested the hypothesis that shifts from meridional to zonal flow across North America, as indicated by the PRGL Index, have been associated with continental-scale hydroclimate variability. We have compiled records of North American paleodroughts from the literature (*SI Text*, Fig. S3, and Table S2) and have identified nine continental-scale droughts that have occurred over the last millennium (Fig. 4). Each of the continental-scale droughts has a particularly strong signature in the Western (W) and SW US. Two large droughts (D13 and D11) have only been observed in Chesapeake Bay and are interpreted here as being East Coast events.

Each of the continental-scale droughts that have occurred over the past millennium is coincident with extreme low years in the PRGL Index, indicating negative PNA years and zonal tropospheric circulation (Fig. 4). With the exception of the 14th century drought, negative PRGL Index values associated with pre-1898 continental droughts vary from −0.91 to −1.29. Similar negative values in 1536 and 1627 are associated with the Chesapeake Bay droughts. The central year for each drought reconstructed by Cook, et al. (34) corresponds well with extreme negative values in the PRGL Index (Fig. 4). For instance, the most negative PRGL Index value occurred in 1152 A.D. This date is consistent with reported dates for the Medieval drought at 1150 A.D. (34) and

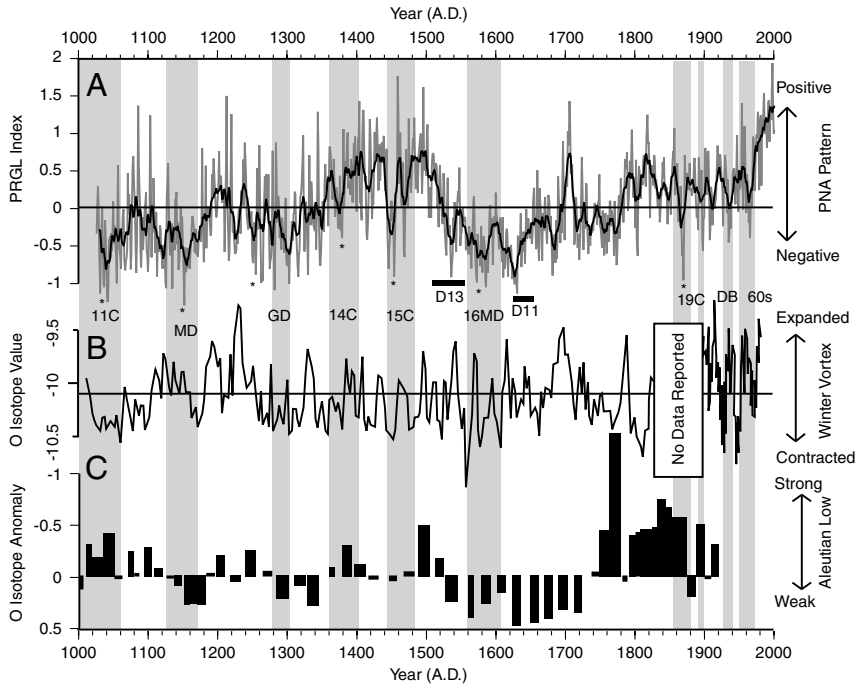


**Fig. 4.** (*A*). Detrended PRGL composite varve record (PRGL values are computed as the mean of the log-transformed PR clastic lamination thicknesses and GL carbonate lamination thicknesses expressed as standard deviation units), with mean value shown with horizontal line. This record is correlated to the PNA pattern, where high values represent positive PNA pattern and low values represent negative PNA values. Previously documented continental-scale droughts (*SI Text*; Fig. S3, Table S2) are illustrated with gray boxes. 11C: 11th century drought; MD: Medieval drought; GD: Great drought; 14C: 14th century drought; 15C: 15th century drought; 16MD: 16th century megadrought; 19C: 19th century droughts (two periods); DB: Dust Bowl; 60s: 1960s drought. D13 and D11 are "dry" intervals (i.e., droughts) identified in Chesapeake Bay (43) but not found in the Western US. Centered age of major droughts reconstructed from the Drought Area Index (34) shown with *. Negative anomalies in the PRGL correspond with known drought periods in North America. Variability in the varve reconstruction of PNA variability is consistent with published records of (*B*). Winter vortex strength (13) and (*C*). The strength of the Aleutian Low (31), further supporting the teleconnection pattern argued for. Horizontal lines in (*A*) and (*B*) Represent the mean value of each series.

1144–1158 A.D. (35), which has been interpreted as the most severe drought in the SW over the past 1,200 y (35). The coincidence between continental droughts and the PRGL Index extreme negative values supports the hypothesis that there is a hydrologic/PNA teleconnection between the NE and other regions of the continent, including the SW.

The three continental-scale droughts that have occurred since 1889 (second period of 19th century drought, Dust Bowl, and 1960s drought) have PRGL Index values that are not as negative as with earlier drought periods (Fig. 4). The reason for this shift over the past century is unclear, however the observation is consistent with recent studies that have demonstrated that 20th Century droughts have been less extreme as compared with droughts earlier in the millennium (34, 35). Based on the results of this study, it is possible that the change in drought severity may be associated with the recent increasing trend observed in the PNA index (29, 32) (Fig. 4).

The mechanism responsible for the teleconnected hydroclimate signal between the NE and SW is likely complex and related to atmospheric and oceanic processes. Drought conditions in the W and SW US have been correlated to La Niña-like conditions in which cool SSTs are present in the eastern tropical Pacific Ocean (34–36). Modeling studies have suggested that the most severe droughts in North America can be explained by cool SSTs in the eastern tropical Pacific Ocean coupled with warm SSTs in the North Atlantic Ocean (37). Both the PNA instrumental record and the PRGL Index reconstruction are significantly correlated with SSTs in the eastern tropical Pacific Ocean (positive) and the North Atlantic Ocean (negative) (*SI Text*, Fig. S1). Therefore, during negative PNA years (low PRGL Index values), SSTs assume a pattern consistent with continental drought conditions in the W and SW US.

## Conclusions

This study has: (*i*) demonstrated that modern varved sediments in the NE preserve hydroclimate conditions; (*ii*) provided evidence that the PNA teleconnection pattern has exhibited a significant control on hydroclimate variability in the region over the late Holocene; (*iii*) produced a high-resolution composite proxy record of the PNA pattern that is consistent with lower-resolution reconstructions of the NE winter vortex and Aleutian Low-pressure system; (*iv*) provided evidence of a recent trend toward enhanced meridional tropospheric circulation that may result in more frequent flooding and less frequent droughts in the NE; and (*v*) demonstrated a teleconnected linkage between NE and W/SW US hydroclimate through a common PNA linkage.

## Methods

Sediment freeze cores ($n = 8$) were analyzed from the Lower Basin of the PR within 20 m of 41°30.11′N × 071°27.04′W in 19.5 m water depth (Fig. 1). Sediment freeze cores ($n = 2$) and surface piston cores ($n = 3$) were analyzed from GL within 40 m of 43°3.02′N × 075°58.01′W in 54.6–54.9 m water depth (Fig. 1).

Continuous and overlapping thin sections were produced and analyzed down each core in order to produce composite varve chronologies from each site (38, 39). Recounts from individual sections yielded counting/chronologic errors of <1%. The PR varve age model has been confirmed using radiometric age constraints (15, 22, 25). The laminated sediments of GL have been confirmed as varved in previous studies (17, 21, 23)

Lamination thickness time series were extracted from the composite varve chronologies and were corrected for differential sediment compaction (25). Turbidites were removed to diminish the effects of episodic physical disturbances. The log transform of each of the PR clastic lamination thicknesses and the GL carbonate lamination thicknesses were converted to standard deviation units, and the mean for each year was computed as the PRGL record.

Lamination thickness time series were compared to instrumental climate records and teleconnection indices using Pearson correlation tests at both annual and decadal (nine-year running average) scales. Precipitation, PDSI,

and temperature values for each state were obtained from the National Oceanic and Atmospheric Administration's National Climate Data Center (40). The PNA was defined here as the EOF2 (December–May) and the NAM as the EOF1 (previous November–December) from the National Centers for Environmental Prediction/ National Center for Atmospheric Research (NCEP/NCAR) reanalysis of sea level pressure from 20°–90 °N (41). The SOI index was defined as the annual average value of the index (42). Correlations were deemed to be significant for $p < 0.05$.

**ACKNOWLEDGMENTS.** The G. Unger Vetlesen Foundation and the National Science Foundation (ATM0354762) provided financial support for this project. Acknowledgment is made to the Donors of the American Chemical Society Petroleum Research Fund for partial support of this research (PRF49438-UNI8). J.B.H. acknowledges support from the Salem State University (SSU) Academic Affairs Office, SSU Dean of Arts and Sciences, K.C.H., J.C.H., and L.T.H. We are grateful for the constructive reviews from the paper's editor and two reviewers.

1. Shiklomanov IA, Rodda JC (2003) *World Water Resources at the Beginning of the 21st Century* (Cambridge University Press, Cambridge) p 435.
2. Mooney H, Cropper A, Reid W (2005) Confronting the human dilemma. *Nature* 434:561–562.
3. Huntington TG (2006) Evidence for intensification of the global water cycle: review and synthesis. *J Hydrol* 319:83–95.
4. Jung M, et al. (2010) Recent decline in the global land evapotranspiration trend due to limited moisture supply. *Nature* 467:951–954.
5. Allen MR, Ingram WJ (2002) Constraints on future changes in climate and the hydrologic cycle. *Nature* 419:224–232.
6. Jones PD, Mann ME (2004) Climate over past millennia. *Rev Geophys* 42:RG2002, doi: 10.1029/2003RG000143.
7. Leathers DJ, Kluck D, Kroczynski S (1998) The severe flooding event of January 1996 across north-central Pennsylvania. *Bulletin of the American Meteorological Society* 79:785–797.
8. Leathers DJ, Grundstein AJ, Ellis AW (2000) Growing season moisture deficits across the northeastern United States. *Clim Res* 14:43–55.
9. Hayhoe K, et al. (2007) Past and future changes in climate and hydrological indicators in the US Northeast. *Clim Dynam* 28:381–407.
10. Hayhoe K, et al. (2008) Regional climate change projections for the Northeast USA. *Mitigation and Adaptation Strategies for Global Change* 13:425–436.
11. Quadrelli R, Wallace JM (2004) A simplified linear framework for interpreting patterns of Northern Hemisphere wintertime climate variability. *J Climate* 17:3728–3744.
12. Bradbury JA, Keim BD, Wake CP (2003) The influence of regional storm tracking and teleconnections on winter precipitation in the northeastern United States. *Ann Assoc Am Geogr* 93:544–556.
13. Kirby ME, Mullins HT, Patterson WP, Burnett AW (2001) Lacustrine isotopic evidence for multidecadal natural climate variability related to the circumpolar vortex over the northeast United States during the past millennium. *Geology* 29:807–810.
14. Orr WL, Gaines AG, Jr (1973) Observations on rate of sulfate reduction and organic matter oxidation in the bottom waters of an estuarine basin: the upper basin of the Pettaquamscutt River (Rhode Island). *Advances in Organic Geochemistry, Proceedings of the 6th International Meeting on Organic Geochemistry*, eds B Tissot and F Bienner (Editions technip, Paris), pp 791–812.
15. Hubeny JB, King JW, Santos A (2006) Subdecadal to multidecadal cycles of Late Holocene North Atlantic climate variability preserved by estuarine fossil pigments. *Geology* 34:569–572.
16. Lincoln SA, Hubeny JB, King JW (2006) A microscopic characterization of varved sediments, Pettaquamscutt River Estuary, RI. *GSA Abstracts with Programs* 38(2):14.
17. Ludlam SD (1984) Fayetteville Green Lake, New York, U.S.A. VII. Varve Chronology and Sediment Focusing. *Chem Geol* 44:85–100.
18. Takahashi T, Broecker W, Li YH, Thurber D (1968) Chemical and isotopic balances for a meromictic lake. *Limnol Oceangr* 13:272–292.
19. Brunskill GJ (1969) Fayetteville Green Lake, New York. II. Precipitation and sedimentation of calcite in a meromictic lake with laminated sediments. *Limnol Oceangr* 14:830–847.
20. Thompson JB, Schultze-Lam S, Beveridge TJ, Des Marais DJ (1997) Whiting events: biogenic origin due to the photosynthetic activity of cyanobacterial picoplankton. *Limnol Oceangr* 42:133–141.
21. Ludlam SD (1969) Fayetteville Green Lake, New York. III. The Laminated Sediments. *Limnol Oceangr* 14:848–857.
22. Hubeny JB, King JW, Cantwell M (2009) Anthropogenic influences on estuarine sedimentation and ecology: examples from the varved sediments of the Pettaquamscutt River Estuary, Rhode Island. *J Paleolimnol* 41:297–314.
23. Wahlen M, Lewis DM (1980) Green Lake: dating of laminated sediments. *EOS* 61:964.
24. Hilfinger MF, IV, Mullins HT, Burnett AW, Kirby ME (2001) A 2500 year sediment record from Fayetteville Green Lake, New York: evidence for anthropogenic impacts and historic isotope shift. *J Paleolimnol* 26:293–305.
25. Hubeny JB (2006) *Late Holocene climate variability as preserved in high-resolution estuarine and lacustrine sediment archives* (University of Rhode Island, Kingston), p 239.
26. Shapley MD, Ito E, Donovan JJ (2005) Authigenic calcium carbonate flux in groundwater-controlled lakes: implications for lacustrine paleoclimate records. *Geochimica et Cosmochimica Ac* 69:2517–2533.
27. Bryson RA, Hare FK (1974) *Climates of North America: volume 11 of World Survey of Climatology* (Elsevier Publishing Co, Amsterdam, New York) p 420.
28. Wallace JM, Gutzler DS (1981) Teleconnections in the geopotential height field during the Northern Hemisphere winter. *Mon Weather Rev* 109:784–812.
29. Leathers DJ, Palecki MA (1992) The Pacific/North American teleconnection pattern and United States climate. Part II: temporal characteristics and index specification. *J Climate* 5:707–716.
30. Hurrell JW, Kushnir Y, Ottersen G, Visbeck M (2003) An overview of the North Atlantic Oscillation. *The North Atlantic Oscillation: climatic significance and environmental impact*, eds JW Hurrell, Y Kushnir, G Ottersen, and M Visbeck (American Geophysical Union, Washington, D.C.), pp 1–35.
31. Anderson L, Abbott MB, Finney BP, Burns SJ (2005) Regional atmospheric circulation change in the North Pacific during the Holocene inferred from lacustrine carbonate oxygen isotopes, Yukon Territory, Canada. *Quaternary Res* 64:21–35.
32. Moore GWK, Holdsworth G, Alverson K (2002) Climate change in the North Pacific region over the past three centuries. *Nature* 420:401–403.
33. Leathers DJ, Yarnal B, Palecki MA (1991) The Pacific/North American teleconnection pattern and United States climate. Part I: regional temperature and precipitation associations. *J Climate* 4:517–528.
34. Cook ER, Woodhouse CA, Eakin CM, Meko DM, Stahle DW (2004) Long-term aridity changes in the western United States. *Science* 306:1015–1018.
35. Woodhouse CA, Meko DM, MacDonald GM, Stahle DW, Cook ER (2010) A 1,200-year perspective of 21st century drought in southwestern North America. *Proc Nat'l Acad Sci USA* 107:21283–21288.
36. Cole JE, Overpeck JT, Cook ER (2002) Multiyear La Niña events and persistent droughts in the contiguous United States. *Geophys Res Lett* 29:25.
37. Feng S, Oglesby RJ, Rowe CM, Loope DB, Hu Q (2008) Atlanticand Pacific SST influences on Medieval drought in North America simulated by the Community Atmospheric Model. *J Geophys Res* 113:D11101.
38. Pike J, Kemp AES (1996) Preparation and analysis techniques for studies of laminated sediments. *Palaeoclimatology and Palaeoceanography from laminated sediments: Geological Society Special Publication No. 116*, ed AES Kemp (Geological Society of London, London), pp 37–48.
39. Francus P, Keimig F, Besonen M (2002) An algorithm to aid varve counting and measurement from thin-sections. *J Paleolimnol* 28:283–286.
40. Guttman NB, Quayle RG (1996) A historical perspective of U.S. climate divisions. *Bulletin of the American Meteorological Society* 77:293–303.
41. Kistler R, et al. (2001) The NCEP-NCAR 50-year reanalysis: monthly means CD-ROM and documentation. *Bulletin of the American Meteorological Society* 82:247–268.
42. Ropelewski CF, Jones PD (1987) An extension of the Tahiti-Darwin Southern Oscillation Index. *Mon Weather Rev* 115:2161–2165.
43. Cronin T, et al. (2000) Climatic variability in the eastern United States over the past millennium from Chesapeake bay sediments. *Geology* 28:3–6.